Application of TPGS as an efflux inhibitor and a plasticizer in baicalein solid dispersion

Meng Tong , Xiaoyan Wu , Shuya Zhang , Di Hua , Shukun Li , Xiangyu Yu , Jing Wang , Zhenhai Zhang

PII: S0928-0987(21)00373-0
DOI: https://doi.org/10.1016/j.ejps.2021.106071
Reference: PHASCI 106071

To appear in: *European Journal of Pharmaceutical Sciences*

Received date: 17 August 2021
Revised date: 7 November 2021
Accepted date: 7 November 2021

Please cite this article as: Meng Tong , Xiaoyan Wu , Shuya Zhang , Di Hua , Shukun Li , Xiangyu Yu , Jing Wang , Zhenhai Zhang , Application of TPGS as an efflux inhibitor and a plasticizer in baicalein solid dispersion, *European Journal of Pharmaceutical Sciences* (2021), doi: https://doi.org/10.1016/j.ejps.2021.106071

Application of TPGS as an efflux inhibitor and a plasticizer in baicalein solid dispersion

Author name: Meng Tong[1], Xiaoyan Wu[2], Shuya Zhang[1], Di Hua[1], Shukun Li[1], Xiangyu Yu[1],Jing Wang[1]*, Zhenhai Zhang[1]*

1. Affiliated Hospital of Integrated Traditional Chinese and Western Medicine, Nanjing University of Chinese Medicine,100 Shizi Road, Nanjing, Jiangsu, 210028, China.

2. Pharmacy, Nanjing Drum Tower Hospital, The affiliated hospital of Nanjing University Medical School, Nanjing, 210008, China.

*Correspondence: Jing Wang
Affiliated Hospital of Integrated Traditional Chinese and Western Medicine, Nanjing University of Chinese Medicine,100 Shizi Road, Nanjing, Jiangsu, 210028, China.
Tel :+86-13675123890
Fax :+86-025-52362115
Email: wangjing3968@126.com

*Correspondence: Zhenhai Zhang
Affiliated Hospital of Integrated Traditional Chinese and Western Medicine, Nanjing University of Chinese Medicine,100 Shizi Road, Nanjing, Jiangsu, 210028,China.
Tel :+86-18913823932
Fax :+86-025-52362115
Email: david23932@163.com

List of abbreviations[1]

Abstract

The oral bioavailability and efficacy of baicalein is dramatically limited by its low solubility and effect of efflux. In our study, we chose PVP-VA64 as a carrier and TPGS as a plasticizer and efflux inhibitor to prepare a solid dispersion of baicalein using hot-melt extrusion technology to improve its solubility and bioavailability. The hot-melt process and formulation were optimized, and a BAC-PVP VA64-TPGS solid dispersion (BPT-SD) was prepared. BAC exists in an amorphous or molecular state in BPT-SD. BPT-SD comprised irregular lumps and small particles without BAC or carrier characteristics. The dissolution efficiency of BPT-SD improved under sink conditions. FTIR showed a strong hydrogen bond between BAC and PVP-VA64 in BPT-SD. BPT-SD maintained good physical stability for 6 months. The apparent permeability coefficient of BAC in the Caco-2 cell model confirmed that BPT-SD had higher gastrointestinal membrane permeability. A rat pharmacokinetic study showed that BPT-SD had higher C_{max} and $AUC_{0\text{-}24h}$, shorter T_{max}, and 2.88-fold higher bioavailability than BAC. A behavioral experiment in chronic unpredictable mild stress (CUMS) mice confirmed the antidepressant efficacy of BAC. BPT-SD reversed

[1]BAC Baicalein
CUMS Chronic unpredictable mild stress
DSC Differential scanning calorimetry
DMEM Dulbecco's modified eagle medium
DMSO Dimethyl sulfoxide
FIIR Fourier Transform infrared spectroscopy
FST Forced swimming test
HBSS Hanks' balanced salt solution
HME Hot-melt extrusion
OFT Open field test
XRD X-ray diffraction
SDS Sodium dodecyl sulfate
SEM Scanning electron microscopy
SPT Sucrose preference test
TST Tail suspension test
TEER Trans-epithelium electrical resistant
Tg Glass transition temperature
TPGS D-α-Tocopherol polyethylene glycol succinate

depression-like behavior in CUMS mice and improved BAC bioavailability. BAC preparation into a solid dispersion significantly enhanced dissolution performance and bioavailability.

Keywords: Baicalein; Solid dispersion; Dissolution; Pharmacokinetics; Chronic unpredictable mild stress

1. Introduction

Baicalein (BAC, structure shown in **Figure 1**) is a natural active phenolic flavonoid compound used in traditional Chinese medicine. It is extracted from the roots of *Scutellaria baicalensis* Georgi (Gao et al., 1999). BAC has antineuritic (X. Zhang et al., 2017), anticancer (Xiaolan Yu et al., 2018), hepatoprotective (H.-L. Huang et al., 2012), antiviral (Zandi et al., 2012), antibacterial (Tang et al., 2015), and antidepressant (LiuLiu, 2017; Ruyi Zhang et al., 2018) properties and other clinically important pharmacological effects. In recent years, BAC has shown great potential for the treatment of depression. According to reports, BAC exerts a neuroprotective effect by regulating the cAMP/PKA, GSK3*β*, NF-κB, and NLRP3 signaling pathways and prevents depression-like behavior induced by chronic unpredictable mile stress (CUMS) (LiuLiu, 2017; C. Y. Zhang et al., 2018; R. Zhang et al., 2018). However, BAC has very low solubility, poor stability, and low oral bioavailability (Huang et al., 2014), which are key factors restricting the pharmaceutical application of BAC.

Solid dispersion technology is an effective method for improving the dissolution rate of poorly soluble drugs. Hot-melt extrusion (HME) technology is a new type of solid dispersion technology that can promote the transformation of the physical state of a raw material drug in a carrier material at the molecular level to form an amorphous system. (Wu et al., 2014) The dissolution rate and apparent solubility are markedly increased, thereby improving oral absorption and bioavailability. For high-melting-point drugs, adding plasticizers is the most effective method to increase the solubility of the raw material. Plasticizers can reduce the viscosity of the extrudate, increase flexibility, lower the operating temperature and Tg of the polymer, and avoid thermal degradation of the drug and carrier (D. Huang et al., 2019). Commonly used plasticizers include surfactants, glycerin, and PEG. Zhang et al (Zhang et al., 2014) prepared a solid dispersion of BAC using HME technology. After oral administration in rats, the relative bioavailability of the two solid dispersion preparations was approximately 2.4 and 2.9 times higher than that of the pure drug, respectively. However, the formulation did not improve the effect of efflux, which may have

affected its bioavailability. TPGS is synthesized by the esterification of vitamin E succinate and polyethylene glycol (PEG) 1000. TGPS is a natural water-soluble derivative of vitamin E and has an amphiphilic structure containing a hydrophilic polar head and a lipophilic alkyl tail. In addition, TPGS can inhibit the efflux of P-glycoprotein and improve the bioavailability of P-glycoprotein blocking drugs (Collnot et al., 2010; Collnot et al., 2007). TPGS can be an excellent solubilizer for hydrophobic drugs (Childs et al., 2013), emulsifiers (Ke et al., 2005), efflux inhibitors (Z. Zhang et al., 2014), plasticizers (Repka, M. A, 2000), and solid dispersion carriers (Beig et al., 2017).

Based on the above discussion, a novel solid dispersion system was prepared to enhance oral bioavailability of BAC using a hot melt extrusion technique with PVP VA64 and TPGS. TPGS was added as an efflux inhibitor and a plasticizer. In vitro and in vivo experiments were carried out to evaluate this solid dispersion system with crystalline BAC as control.

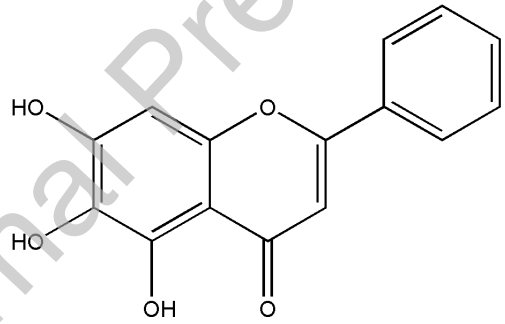

Figure 1. Structural formula of BAC

2. Materials and methods

2.1 Materials

BAC (purity > 95%) was purchased from Aladdin Bio-Chem Technology Co., Ltd. (Shanghai, China). PVP VA64 and TPGS were kindly supplied by Chineway Pharmaceutical Tech. Co. Ltd. (Shanghai, China). Fluoxetine hydrochloride (FLU) (positive control drug) was obtained from Changzhou Siyao Pharmaceuticals Co., Ltd. (Changzhou, China). All other chemicals were of analytical grade.

2.2 Animals

Male Sprague–Dawley (SD) rats (220 ± 20 g) used in the pharmacokinetic study

were purchased from the SLAC Lab Animal Center of Shanghai (Shanghai, China) and allowed to acclimate to the environment for 7 days prior to the experiments.

Male BALB/c mice (20 ± 2 g), which were used for CUMS, were purchased from the Yangzhou University Comparative Medical Center (Yang Zhou, China) and allowed to acclimate to the environment for 2 weeks prior to CUMS induction.

All animal experiments were reviewed and approved by the Institutional Animal Care and Use Committee of the Jiangsu Provincial Academy of Chinese Medicine. License number: SCXK (Su) 2018-0018

2.3 Preparation of BPT-SD

Based on our preliminary experiments, we selected Kollidon® VA64 to prepare BAC solid dispersion. HME was conducted using a Process 11 twin-screw hot-melt extruder (Thermo Electron Corporation, MA,USA). Importantly, the operations were conducted in the dark because BAC is photolabile when exposed to light. We designed an orthogonal experiment to optimize the hot-melt preparation process parameters and formulas.

2.4 *In vitro* dissolution study

2.4.1 Equilibrium solubility test

We added excess BAC to the pH 1.2 hydrochloric acid solution and pH 6.8 phosphate buffer solution containing different proportions of SDS , equilibrated in a shaker at 37 °C for 48 h. The equilibrium solution was transferred to a centrifuge tube and centrifuged at 13,000 ×g for 10 min. The supernatant was removed and measured according to the chromatographic conditions. All samples were tested in triplicate.

2.4.2 Dissolution test

The dissolution of pure BAC powder, BAC-PVP VA64-TPGS physical mixture (BPT-PM), and BAC-PVP VA64-TPGS solid dispersion (BPT-SD) were examined using a ZRS-8GD dissolution apparatus (Tianfa Technology, China) at a paddle rotation speed of 50 ×g.

Samples equivalent to 15 mg of BAC were accurately weighed and added to 900 mL dissolution solution at 37 °C. Two milliliters of the sample were withdrawn at

different time points (5, 10, 15, 30, 45, 60, 75, 90, and 120 min) and filtered through 0.45 μm polyester filters. Another 2 mL of fresh dissolution fluid was added to maintain a constant dissolution volume. The filtrate was subjected to HPLC quantification using an Agilent HPLC system (LC 1100, Agilent, La Jolla, CL, USA). Each test was performed in triplicate.

Chromatographic separation was conducted on the Agilent HPLC system (Agilent Corporation) equipped with an ultraviolet absorbance detector set at 276 nm. The separation was performed at 30 °C on an X-Bridge C_{18} column (5 μm, 250 mm × 4.6 mm, Waters Corporation, USA). The mobile phase consisted of methanol: 0.1% phosphoric acid (65/35, v/v). The mobile phase was freshly prepared prior to each series of analyses. The retention time was 6.8 min, and the total run of each sample was 10 min.

2.5 Physical characterization of BPT-SD

2.5.1 DSC

DSC was performed to characterize the state of the drug in the solid dispersion using a 200F3 instrument (NETZSCH, Germany). Approximately 8 mg of each sample was placed in an aluminum pan. The measurements were conducted at a heating rate of 10 °C/min from 30 °C to 300 °C (Zhang et al., 2014).

2.5.2 XRD

X-ray diffraction (XRD) was conducted using a Bruker-D8 X-ray diffractometer (Bruker Corporation, Germany). The samples were exposed to Cu Kα radiation (40 kV, 40 mA) over a 2θ range from 5° to 90°, with a step size of 0.04° and a step time of 0.5 s.

2.5.3 SEM

SEM measurements were conducted with a ZEISS-SUPRA40 electron microscope (ZEISS Co., Germany) at 15 kV and 15 μA. The samples were coated with gold prior to the measurements.

2.5.4 FTIR

Fourier transform infrared spectroscopy (FTIR) was performed using a Bruker IFS-55 interferometer (Bruker, Germany). The samples were ground and mixed

thoroughly with potassium bromide (KBr). Then, they were compressed into tablets for scanning at a resolution of 4 cm^{-1} and a range of 400 to 4000 cm^{-1} (Wang et al., 2017).

2.6 Solubility test

We added excess BAC, BPT-PM, and BPT-SD to the hydrochloric acid buffer solution containing 0.5% SDS at pH 1.2, equilibrated in a shaker at 37 °C for 48 h. The equilibrium solution was transferred to a centrifuge tube and centrifuged at 13,000 ×g for 10 min. The supernatant was removed and measured according to the aforementioned chromatographic conditions (Zhang et al., 2014). All samples were tested in triplicate.

2.7 Stability study

When exposed to environments of high humidity or high temperature, the physiochemical properties of BPT-SD may deteriorate. We evaluated the long-term stability of BPT-SD. The BPT-SD powder packaged in an airtight container was stored at 40 ± 2 °C and 75 ± 5% relative humidity. After 6 months, the dissolution and XRD were examined and compared with the original state (Nepal et al., 2010). All samples were tested in triplicate.

2.8 Caco-2 cell transport experiment

2.8.1 Caco-2 cell culture

The human colon carcinoma cell line Caco-2 was used to study BAC transport. Briefly, Caco-2 cells were stored in an incubator at 37 °C, with 95% relative humidity, and 5% CO_2. Caco-2 cells were seeded at a density of approximately 1×10^4 cells/cm^2 in 24-well Transwell® plates to reach confluence and differentiation. At 21 days post-seeding, the cells developed well with TEER values greater than 600 Ω·cm^2 (Xiaoyan et al., 2017).

2.8.2 Cytotoxicity of BPT-SD

In the CCK-8 assay, the dye of WST-8 [2-(2-methoxy-4-nitrophenyl)-3-(4-nitrophenyl)-5-(2,4disulfophenyl)-2H-tetrazolium, monosodium salt] is reduced by cellular dehydrogenase to form a water-soluble orange-colored product (formazan) (Cai et al., 2019). The CCK-8 assay was performed as described previously by Li et

al. (2020) with some modifications. Caco-2 cells were incubated in high-glucose and L-glutamine DMEM supplemented with 1% (v/v) penicillin-streptomycin and 10% (v/v) fetal bovine serum. The cells were seeded at a density of 2.5×10^4 cells/well in 96-well plates and incubated at 37 °C and 5% CO_2 for 72 h. The culture medium was removed, and BAC was dissolved in DMSO. This solution was then diluted to different concentrations (1.01–40.4 μg/mL) by adding DMEM to the wells where the DMSO dosage was less than 0.5%. After 24 h of incubation, the cells were washed three times with 200 μL PBS/well (Shen et al., 2018). Then, 200 μL CCK-8 containing medium (5 mg/mL CCK-8 in DMEM) was added to dissolve the formazan crystals, and absorbance was measured at 570 nm using a microplate reader (Synergy HT, BioTek, USA). Relative cell viability (%) was calculated by comparing the absorbance of the treated cells with that of control cells (Slütter et al., 2009).

2.8.3 Transport experiment

The transport assay was performed in the apical–basolateral direction. The test solutions of BAC, BAC+PVP VA64, and BAC+PVP VA64+TPGS1000 at doses of 1, 5, and 20 μg/mL of BAC were prepared by adding the appropriate amount of each formulation to DMSO and diluted with the Hanks' balanced salt solution (HBSS, pH 7.4) to corresponding concentration. Caco-2 cell monolayers were washed twice with prewarmed HBSS before permeability studies. The experiments were initiated by adding 0.5 mL of the test solution to the apical chamber (AP) and 1.5 mL of HBSS to the basolateral chamber. The plates were agitated on an orbital shaker at 50 ×g throughout the incubation period. Samples (150 μL) were then taken from the basolateral chamber and immediately replaced with the same volume of HBSS at 37 °C and predetermined time intervals of 30, 60, 90, and 120 min. The samples were stored at -20 °C until analysis.

The concentration of BAC in the transport buffer samples was determined using HPLC analysis. The apparent permeability coefficient (Papp) across the Caco-2 cell monolayer was calculated for permeability studies using the following equation:

$$\text{Papp}=\left(\frac{dQ}{dt}\right)\left(\frac{1}{AC_0}\right)$$

where dQ/dt (μg/min) is the transport rate, A is the surface area of the monolayer, and C_0 is the initial concentration of BAC (μg/mL).

2.9 Pharmacokinetic study

2.9.1 Animal experiment

For the pharmacokinetic study, SD rats (180–220 g) were randomly divided into three groups (n = 8). Briefly, BAC, BPT-PM, and BPT-SD (dispersed in 0.5% aqueous sodium carboxymethyl cellulose) were orally administered at a dose of 75 mg/kg (Liu et al., 2006). Blood samples were collected in heparinized tubes from the orbital vein at predetermined times (0, 5, 15, 30, 60, 120, 180, 240, 300, 360, 480, 600, 720, and 1440 min) after oral administration. Blood samples were immediately centrifuged at 13,000 ×g for 10 min to obtain plasma.

2.9.2 Plasma sample preparation

Plasma (150 μL) and internal standard solution (Daidzin, 50 μL) were spiked with 400 μL of methanol, followed by vigorous vortexing for 5 min to precipitate the plasma proteins. The samples were centrifuged at 16,000 ×g for 10 min at 4 °C. After centrifugation, 20 mL of the supernatant was injected into the HPLC system to determine BAC concentration. (Lai et al., 2003)

After oral administration of baicalein, a prototype drug baicalein, in rats, was almost completely metabolized after 2 h, and the detectable drug concentration was extremely low. Baicalin is the main form of BAC after being absorbed and metabolized in the body; therefore, baicalin was chosen as the test index (Pan et al., 2013).

2.9.3 HPLC analysis of plasma samples

For the stationary phase, an Agilent C18 column (250 mm × 4.6 mm, 5 μm) was maintained at 25 °C. The mobile phase comprised a mixture of 0.1% H_3PO_4 and acetonitrile, which was run in a gradient elution program. The flow rate was 1.0 mL/min.

2.10 Effect of BPT-SD in CUMS mouse model

2.10.1 CUMS and experimental design

A total of 84 BALB/c mice were randomly assigned to seven groups of 12 mice

each, using a randomization method. The groups were Control, CUMS, CUMS-FLU (10 mg/kg), CUMS-BAC (20 and 40 mg/kg), and CUMS-SD (20 and 40 mg/kg) (Zhang et al., 2018). The CUMS procedure was conducted as previously described (Willner et al., 1987) with slight modifications. The specific details of the CUMS procedure are as follows: (1) cage shaking (1 time/s, 10 min); (2) cage tilt (45°, 8 h); (3) food and water deprivation (24 h); (4) soiled cage (200 mL water in 100 g sawdust bedding); (5) overnight illumination (8 h); (6) restrained in a bottle; (7) tail pinched (1 cm from the beginning of the tail); (8) light/dark perversion; (9) stroboscopic illumination (120 flashes/min, 1 h); and (10) cold water swimming (4 °C, 5 min). Each animal was individually exposed to one stressor per day. The control animals (n = 12) were housed in a separate room and had no contact with the stressed animals.

After the fourth week of the CUMS paradigm, when depressive-like behaviors occurred, drugs were administered once per day during the last 15 days. Behavioral tests were performed 1 h after the final drug administration.

2.10.2 Behavioral tests

Sucrose preference test (SPT) was performed using the traditional method, with minor modifications. Briefly, before initiating the CUMS procedure, the mice were individually housed. Two bottles of 1 m/v% sucrose solution were placed in each cage for 24 h to allow the mice to adapt to the solution. Then, one bottle of sucrose solution was replaced with water (24 h). The mice were deprived of food and water for 8 h before the test and only provided two bottles with 1% sucrose solution and water for 2 h.

Sucrose preference (%) = [sucrose consumption (g)/water consumption (g) + sucrose consumption (g)] × 100%

The goal of the open field test (OFT) was to observe the autonomous behavior, exploratory behavior, and tension of experimental animals in a new environment and evaluate the level of anxiety in the experimental animals. The open field apparatus was 39 × 39 × 40 cm and divided equally into nine sections (13 × 13 cm). The mice were individually placed in the center of the cage in a quiet environment. After 2 min

of adaptation, the mice were allowed to explore freely during a 4-min testing period, and the total distance was recorded (LiuLiu, 2017).

The forced swimming test (FST) was performed to evaluate depressive-like behavior according to the time of immobility. The mice were placed in a cylinder (25 cm high, 10 cm diameter) filled with 19 cm of water at 25 ± 1 °C. On the first day, the rats or mice were forced to swim in deep water at 25 °C for 15 min and then returned to the cage. After being forced to swim for 6 min the next day, the immobility time was recorded during the last 4 min of the test. There was no chronological effect in the swimming experiment; that is, the results of the experiment at different times of the day were consistent (Chen-Yi-Yu et al., 2018).

The tail suspension test (TST) reflected the desperate behavior of mice and was used to detect variability in animal behavior. The mouse was fixed on a tail suspension instrument approximately 35 cm from the ground and held head downward. The duration of the test was 6 min, and the immobility time, defined as the time when the mouse was completely immobile, was recorded during the last 4 min of the test (Li et al., 2015; Zhang et al., 2018).

2.11 Statistical analysis

Data are presented as mean ± standard error of the mean for all data. The data processing software DAS 3.0 (Mathematical Pharmacology Professional Committee of China, Shanghai, China) was used to calculate the pharmacokinetic parameters. Statistical software (SPSS 22.0, SPSS Inc., Chicago, IL, USA) was used for analyses. Statistical analyses were performed using one-way ANOVA. If the distribution was normal, Student's *t*-test was also used. If the distribution was not normal, the Wilcoxon rank-sum test was used. $p < 0.05$ indicated statistically significant differences.

3. Results and Discussion

3.1 Preparation of BPT-SD

In this study, we prepared a solid dispersion of BAC using HME technology, and the formulation and process were optimized using an orthogonal design. DSC, XRD, SEM and FTIR analysis and pharmaceutical research including solubility,

dissolution , permeability , bioavailability and pharmacodynamics were studied to characterize the particles obtained by HME process (Kim et al., 2008) . In the pre-experiment , we selected different carriers according to the literature (Zhang et al., 2014 ;Li et al., 2017). Finally, PVP VA64 was selected as the preferred carrier because of its good solubility and stability. Because of the high melting point of BAC (approximately 265 ℃), we considered adding a plasticizer to improve the compatibility of BAC and the carrier PVP VA64 (D. Huang et al., 2019). The Hansen solubility parameters reflect the degree of mixing between the drug and its corresponding carrier. The solubility parameter value of BAC was 17.2 $Mpa^{1/2}$, and the difference Δδ between PVP-VA64 was less than 7 $Mpa^{1/2}$, indicating that it may be compatible with BAC (Fule et al., 2016).

Using the cumulative dissolution rate at 15 min as an indicator and comparing the solid dispersions under different processes, the final optimal process was as follows: speed was 50 ×g, temperature in zones 2–8 was 140–170 °C, and the ratio of BAC to carrier was 1:6, which contained 10% TPGS. This is a novel solid dispersion system prepared using the HME technique with a hydrophilic polymer and plasticizer, without an organic solvent.(Adler et al., 2016)

3.2 In *vitro* dissolution study

3.2.1 Equilibrium solubility test

We carried out an equilibrium solubility test during the prescription screening phase. The results are shown in **Table 1**. BAC is a chemical component with low solubility. We found that the equilibrium solubility of BAC in ph1.2 and ph6.8 dissolution media was only 6.49±1.60 and 6.40±0.84 μg/ml respectively which was difficult to reach the sink condition. Therefore, SDS was selected to improve the solubility of BAC. After screening, 0.5% SDS was added into the dissolution medium which not only met the sink condition, but also reached the limit of detection. Referring to Zhang et al ' s research (Zhang et al., 2014), we finally chose 0.5 % SDS.

Table 1. Equilibrium solubility of BAC in different dissolution media

Dissolution medium	Equilibrium solubility(μg/ml)
pH 1.2 buffer	6.49±1.60

pH 1.2+0.1%SDS	13.70±0.71
pH 1.2+0.3%SDS	36.83±0.33
pH 1.2+0.5%SDS	59.58±1.81
pH 6.8 buffer	6.40±0.84
pH 6.8+0.1%SDS	9.64±2.20
pH 6.8+0.3%SDS	29.57±1.61
pH 6.8+0.5%SDS	59.72±0.39

3.2.2 Dissolution test

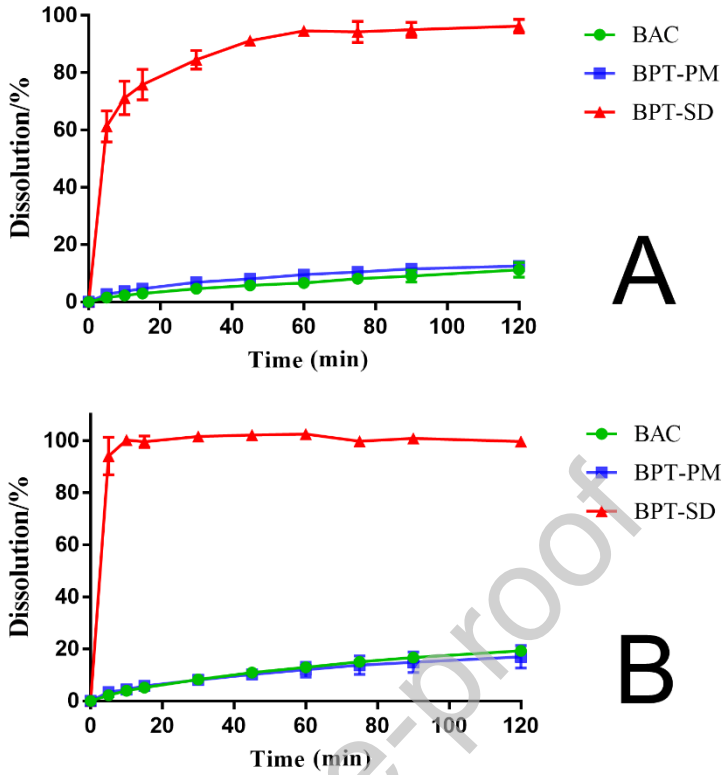

Figure 2. Dissolution curves of pure BAC, BAC-PVP VA64 PMs, and BAC-PVP VA64 SDs at different pH values (A pH 1.2; B pH 6.8) under sink conditions (n = 3)

As shown in **Figure 2**, in the hydrochloride buffer containing 0.5% SDS **(Figure 2.A)**, the bulk drug and physical mixture showed less than 10% dissolution in 15 min, and 11.2% and 12.53% dissolution, respectively, in 120 min. The dissolution of BPT-SD in 15 min was 75.89%; after 30 min, it exceeded 80% and reached 96.26% in 120 min. In the phosphate buffer containing 0.5% SDS **(Figure 2.B)**, the dissolution of BAC and BPT-PM in 5 min was less than 5%, and the dissolution in 120 min was less than 20%. The BPT-SD dissolved in 5 min. The dissolution rate exceeded 90% within 120 min. It can be seen that under this process, the dissolution efficiency of BAC was greatly improved.

3.3 DSC

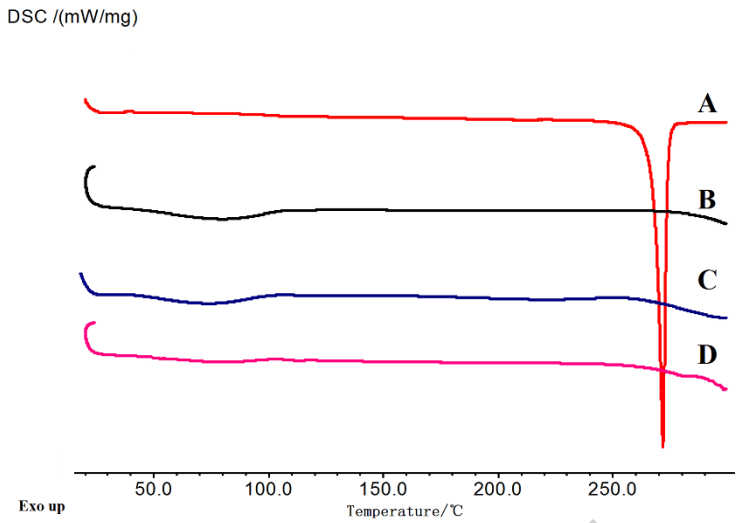

Figure 3. DSC thermograms of BAC (A), PVP VA64 (B), BPT-PM (C), and BPT-SD (D)

DSC is mainly used to detect whether the crystal form of BAC changes during the preparation of solid dispersions(Zhang et al., 2014). As shown in **Figure 3**, BAC **(Figure 3.A)** has a sharp endothermic peak at 271.6 °C, which is the characteristic peak of the melting point of BAC. PVP VA64 **(Figure 3.B)** showed no significant endothermic peaks. BPT-PM **(Figure 3.C)** also showed no obvious endothermic peak, which may be due to the drug being dissolved in the carrier at a high temperature. There was no significant endothermic peak in BPT-SD **(Figure 3.D)**, and the drug was present in the carrier in an amorphous or molecular state (Wang et al., 2019)

3.4 XRD

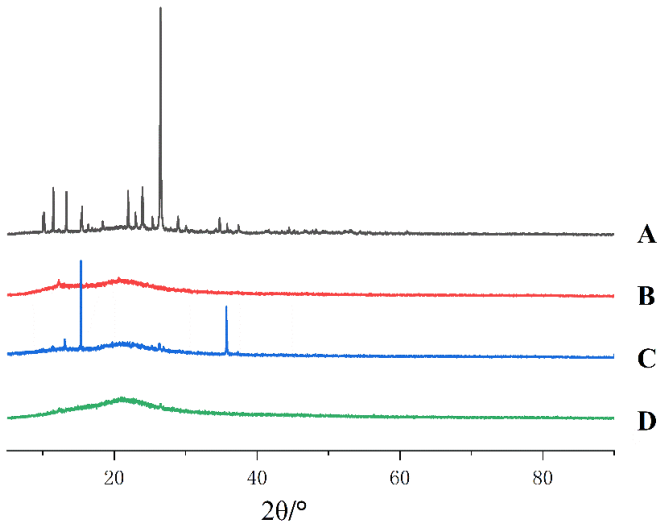

Figure 4. XRD patterns of BAC (A), PVP VA64 (B), BPT-PM (C), and BPT-SD (D)

XRD was used to determine the crystallinity of different samples. As shown in **Figure 4**, BAC **(Figure 4.A)** has multiple crystal diffraction peaks at 10.14°, 11.34°, 13.22°, 15.32°, 26.30°, and 34.02° (Wen et al., 2018). PVP VA64 **(Figure 4.B)** did not show obvious crystal diffraction peaks, indicating that PVP VA64 was in an amorphous or molecular state. BPT-PM **(Figure 4.C)** showed the diffraction peak of BA, but it was weakened by the mixing of some polymers, which indicated that the physical mixture was simple. However, the XRD patterns of the solid dispersions **(Figure 4.D)** did not show the crystal diffraction peak of BAC, indicating that the crystalline nature of BAC disappeared. Based on the DSC results, it is speculated that BAC was dispersed in the solid dispersion in an amorphous or molecular state. (He et al., 2011)

3.5 SEM

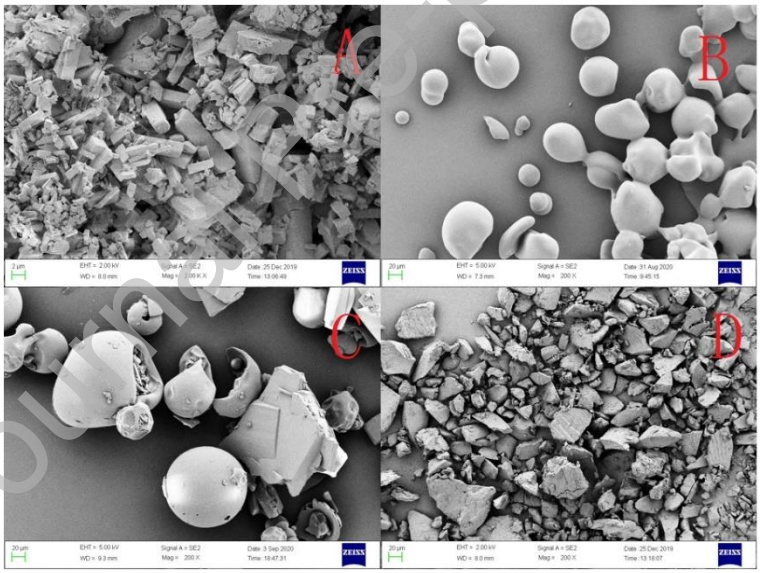

Figure 5. SEM images of BAC (A), PVP VA64 (B), BPT-PM (C), and BPT-SD (D)

SEM was used to observe the surface and crystal structures of BAC, BPT-PM, and BPT-SD. The results are presented in **Figure 5**. BAC **(Figure 5.A)** mostly had columnar crystals accompanied by large lumps with obvious crystal characteristics. PVP VA64 **(Figure 5.B)** had a smooth spherical or ellipsoidal shape. The characteristics of BAC and PVP VA64 were clearly visible in BPT-PM **(Figure 5.C)**. BPT-SD **(Figure 5.D)** had no raw material characteristics, consisting primarily of

irregularly shaped blocks with granular, loose, and porous surfaces (Fan et al., 2020).

3.6 IR

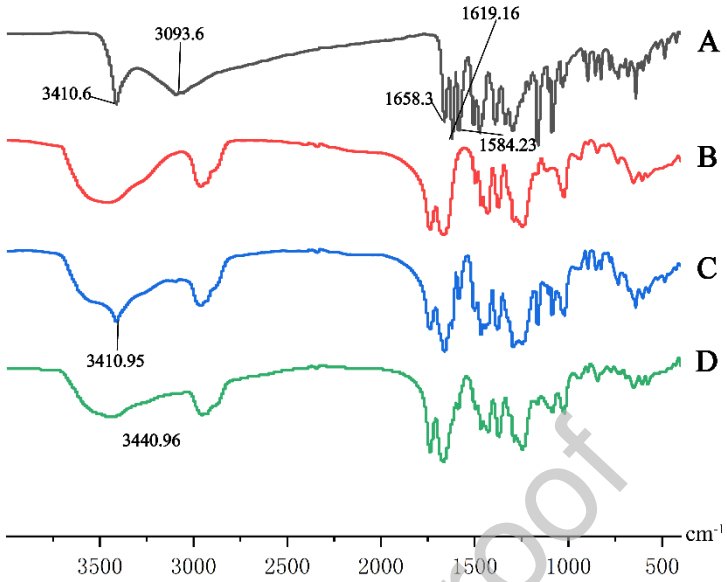

Figure 6. FTIR results of BAC (A), PVP VA64 (B), BPT-PM (C), and BPT-SD (D)

FTIR was used to study the possible interactions between BAC and the polymer. The results are shown in **Figure 6.** In the FTIR spectrum of BAC crystals, the band at 3,410.6 cm^{-1} corresponded to the OC–H stretching vibrations of the hydroxyl group, indicating the intramolecular hydrogen bonds of BAC. The absorption peak at 3,093.6 cm^{-1} for the binding peaks was derived from the intermolecular hydroxyl group, and the peaks at 1,658.3 , 1,619.16, and 1,584.23 cm^{-1} （Zhang et al., 2014）were caused by the absorption of the benzene ring.

In BPT-PM, the characteristic peaks at 3,410.95 cm^{-1} of BAC were clearly observed, indicating that simple physical mixing resulted in no interactions between BAC and the polymer. However, in BPT-SD the broadened peak at 3,410.95 cm^{-1} of BAC was weakened and shifted to the left at 3440.96 cm^{-1}, which indicated intermolecular hydrogen bonds between the drug and carrier after HME (Huang et al., 2014; Wen et al., 2018)

3.7 Solubility test

Table 2. Solubility of BAC and solid dispersions (n = 3)

Sample	Solubility/μg mL^{-1}
BAC	40.28 ± 2.08
BPT-PM	43.31 ± 1.28
BPT-SD	316.07 ± 20.50**

Compared with BAC, $^{**}p < 0.01$

The solubilities of BAC, physical mixture, and solid dispersion are shown in **Table 2**. The equilibrium solubility of BAC was 40.28 μg·mL^{-1} and BPT-PM was 43.31 μg·mL^{-1}. However, the solid dispersion with PVP-VA64 as a carrier greatly improved its solubility, which was 7.85 times higher ($p < 0.01$) because of the presence of a hydrophilic carrier. After the preparation of BPT-SD, its molecular order was disrupted; it had a larger surface energy, and the contact area between BAC and the medium increased, resulting in greater solubility.

3.8 Preliminary stability study

3.8.1 *In vitro* dissolution study

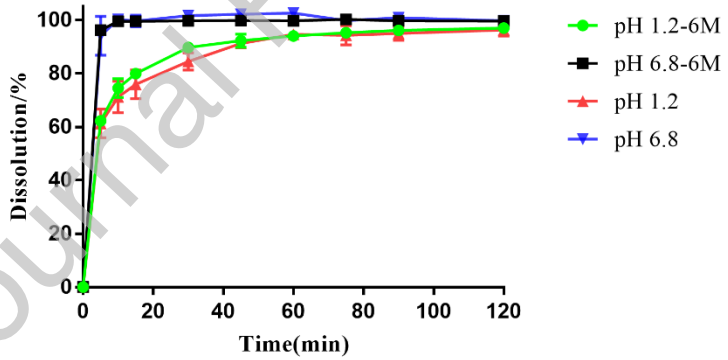

Figure 7 Dissolution curves of BAC at different pH values under the accelerated condition

The stability results are presented in **Figure 7**. After 6 months, the dissolution of BPT-SD was consistent with the original curve, indicating that BPT-SD could maintain stability for at least 6 months. It is possible that in the solid content, BAC interacts with PVP VA64 and TPGS could play a plasticizing effect, further increasing its stability and theoretically reducing crystals and amorphous or molecular solids (Huang et al., 2019)

3.8.2 XRD

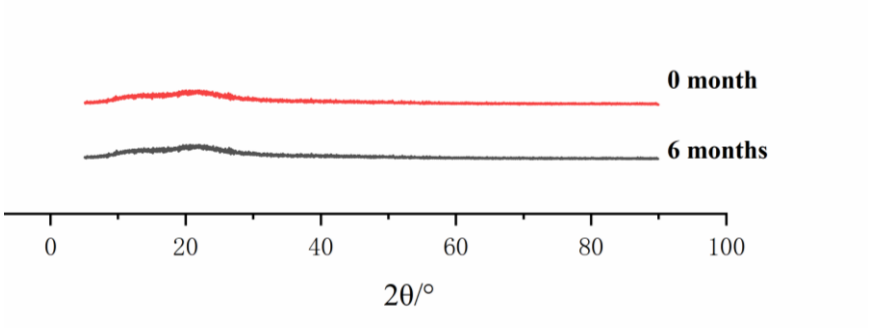

Figure 8. XRD of BAC under accelerated conditions

Physical stability is an important issue in thermodynamically unstable systems. The free energy of amorphous or molecular crystals is higher than that of stable crystals. Therefore, XRD was used to study the physical stability of amorphous or molecular drugs in SD rats. As shown in **Figure 8**, after 6 months of accelerated stability experiments, the XRD of BPT-SD did not show a new diffraction absorption peak, indicating that BAC and PVP VA64 still existed in an amorphous or molecular state and exhibited good physical stability.

3.9 Caco-2 cell transmembrane transport results

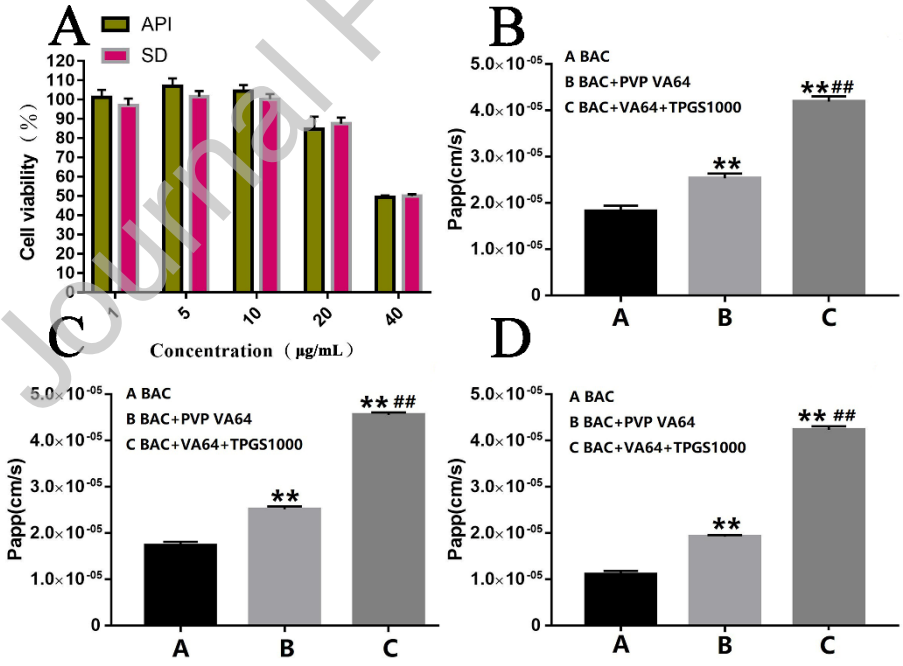

Figure 9. Results of cell cytotoxicity (A) and the effect of BPT-SD (B. 5 μg/mL; C. 10 μg/mL; D. 20 μg/mL) on the apparent permeability coefficient of BAC across Caco-2 monolayer (n = 3).*p < 0.05, **p < 0.01, compared to BAC, $^{\#\#}p$ < 0.01, compared to BAC-PVP VA64.

3.9.1 Cytotoxicity assessment

The CCK-8 method was used to determine the cytotoxicity of BAC and BPT-SD in Caco-2 cells at different concentrations. As shown in **Figure 9.A**, after 24 h of measurement, the survival rate of Caco-2 cells in the test group treated with 1, 5, 10, and 20 μg/mL was greater than 80%, indicating that BAC and BPT-SD were not toxic to Caco-2 cells in this concentration range. Based on the results of the CCK-8 experiments, BAC concentrations of 5, 10, and 20 μg/mL were selected to conduct drug transport experiments across the membrane.

3.9.2 Transmembrane transport results

According to previous reports, BAC can upregulate the expression of P-glycoprotein in Caco-2 cells and affect its transport activity. TPGS inhibits the efflux of P-glycoprotein and improves the bioavailability of P-glycoprotein blocking drugs (Collnot et al., 2010); therefore, we considered adding TPGS to improve the transmembrane transport capacity of BAC.

The results of the BAC and BPT-SD transfers are shown in **Figure 9**. The transport results (**Figure 9.B**) showed that the Papp values of 20 μg/mL BAC, BAC-PVP VA64, and BAC-PVP VA64-TPGS were 1.126×10^{-5}, 1.966×10^{-5}, and 4.231×10^{-5}, respectively. The Papp values of BAC-PVP VA64 and BAC-PVP VA64-TPGS were significantly increased ($p < 0.01$) by 1.75- and 3.76-fold, respectively, compared with that of BAC. In addition, the Papp values of 10 μg/mL of BAC-PVP VA64 and BAC-PVP VA64-TPGS were increased by 1.46- and 2.64-fold ($p < 0.01$) **(Figure 9.C)**, and the Papp values of 5 μg/mL B and C were increased by 1.4- and 2.31-fold ($p < 0.01$) **(Figure 9.D)**. This showed that the preparation process of the solid dispersion could effectively improve the cell membrane permeability of BAC. Compared with B, the Papp value of C was significantly increased ($p < 0.01$), indicating that TPGS inhibited the transport of P-glycoprotein and increased the concentration of the drug. Moreover, the resistance value of the Caco-2 cell membrane did not change significantly before and after the experiment, indicating that the integrity of the cell membrane did not change during the experiment.

3.10 Pharmacokinetic study

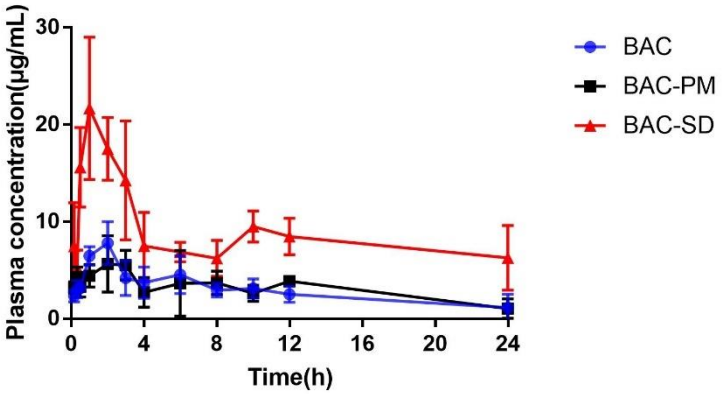

Figure 10. Plasma concentration-time profiles of pure BAC and BPT-SD at a 1:6 ratio and BPT-PM at a 1:6 ratio in rats following oral administration (n = 6)

Table 3. Pharmacokinetic parameters of drugs in mice after oral administration of BAC, BPT-PM, and BPT-SD (n = 6)

Parameter	BAC	BPT-PM	BPT-SD
C_{max} (μg/mL)	8.13 ± 1.15	6.97 ± 1.90	23.09 ± 5.79**
T_{max} (h)	1.50 ± 0.58	1.87 ± 0.96	1.10 ± 0.55
$AUC_{0\text{-}24h}$ (μg/mL·h)	71.97 ± 26.92	98.67 ± 33.57	207.4 ± 27.36**

Compared with BAC, * $p < 0.05$, ** $p < 0.01$

Based on the drug-time curve (**Figure 10**) and the pharmacokinetic parameter table (**Table 3**), after intragastric administration, the T_{max} of the BAC group was 1.5 ± 0.58 h, C_{max} was 8.13 ± 1.15 μg/mL, and $AUC_{0\text{-}24h}$ was 71.97 ± 26.92 μg·h/L. The T_{max} of the BPT-SD group was 1.1 ± 0.55 h, C_{max} was 23.09 ± 5.79 μg/mL, and $AUC_{0\text{-}24h}$ was 207.4 ± 27.36 μg·h/L. Compared with the BAC group, the BPT-PM group did not show significant increase in C_{max} and $AUC_{0\text{-}24h}$. The C_{max} and AUC of the BPT-SD group significantly increased ($p < 0.01$) by 2.84- and 2.88-fold, respectively. Therefore, the preparation of BAC into a solid dispersion could significantly improve the bioavailability of BAC.

The results of the pharmacokinetic test of BAC showed that baicalin had a double peak phenomenon with baicalin as the detection index (Lai et al., 2010). After oral administration, BAC is directly absorbed in the intestine and catalyzed by glucuronyl transferase (UGT) to generate baicalin, which enters the blood circulation, thus forming the first peak. Baicalin in the blood passes through the hepato-intestinal

circulation and is metabolized into BAC in the intestine through the flora and subsequently absorbed (Kotani et al., 2006). The absorbed baicalin is again glucuronated in the body and excreted by the small intestine, thus forming the second peak.

3.11 Effects of BAC on depressive-like behaviors

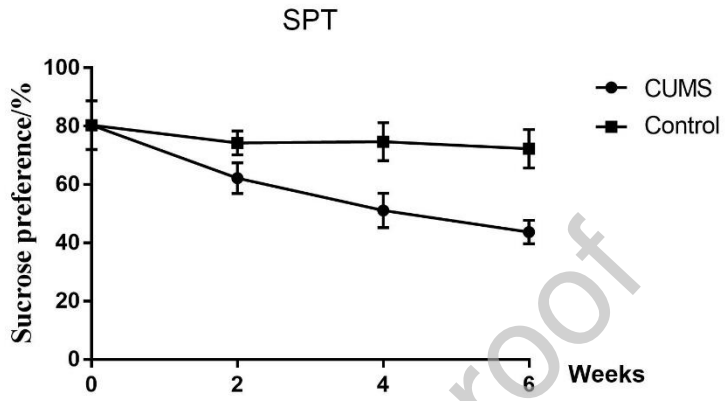

Figure 11. Sucrose preference of the Control group and CUMS group over 6 weeks (n = 8)

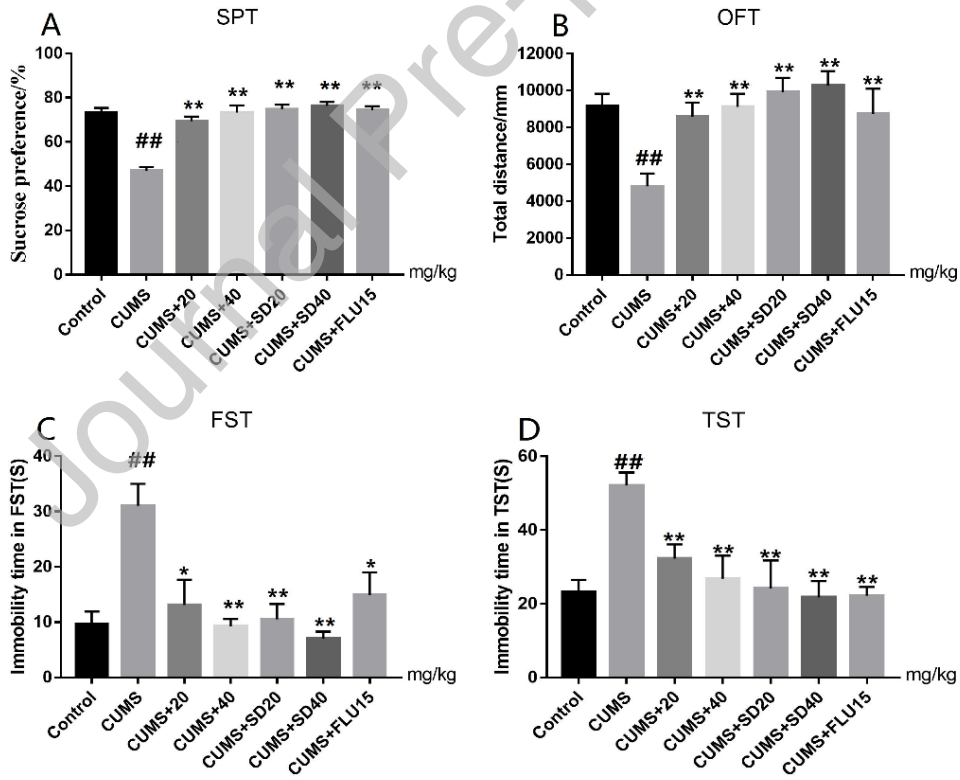

Figure 12. Effects of BAC on sucrose preference index in SPT (A), total distance in OFT (B), and immobility time in FST (C) and TST (D) in CUMS mouse model. Results are shown as the mean ± SD (n=12). $^{\#\#}p < 0.01$ versus the Control group; $^{*}p < 0.05$, $^{**}p < 0.01$ versus the CUMS group.

BAC (20mg/kg) could maintain neuronal survival, promote neuronal maturation,

and rescue neurons from apoptosis via inhibiting activation of GSK3β/NF-κB/NLRP3 signal pathway that is known to be associated with inflammation, thus exerting neuroprotective effects and preventing CUMS-induced depressive-like behaviors.(Zhang et al., 2018) Lack of anhedonia is a typical symptom of depression. As shown in **Figure 11**, after 4 weeks of CUMS, the sugar water preference of CUMS mice decreased significantly ($p < 0.01$), indicating that the model was successful.

3.11.1 SPT

As shown in **Figure 12.A**, compared with the blank group, the sucrose consumption in the CUMS group significantly reduced ($p < 0.01$). However, BAC (20 and 40 mg/kg), BPT-SD (20 and 40 mg/kg), and the positive drug FLU reversed the change in sucrose preference. The reversal effect of BPT-SD was slightly higher than that of BAC but not substantial.

3.11.2 OFT

Compared with the blank group, the total exercise distance of the CUMS group was significantly reduced, which indicated that the exercise capacity of the CUMS group was significantly reduced. As shown in **Figure 12.B**, compared with the CUMS group, BAC (20 and 40 mg/kg), BPT-SD (20 and 40 mg/kg), and FLU (15 mg/kg) significantly improved exercise capacity. Among them, the exercise capacity between the BPT-SD-treated group and the blank group did not change significantly ($p > 0.05$), indicating that it would not cause excitability of the central nervous system.

3.11.3 FST

As shown in **Figure 12.C**, compared with that in the blank group, the immobility time in the CUMS group was significantly increased. BAC (20 and 40 mg/kg, $p < 0.05$, $p < 0.01$), BPT-SD (20 and 40 mg/kg, $p < 0.01$), and FLU (15 mg/kg, $p < 0.05$) significantly reduced the immobility time.

3.11.4 TST

As shown in **Figure 12.D**, compared with that in the blank group, the immobility time in the CUMS group significantly increased. BAC (20 and 40 mg/kg, $p < 0.01$), BPT-SD (20 and 40 mg/kg, $p < 0.01$), and FLU (15 mg/kg, $p < 0.01$) significantly reduced immobility time.

In summary, these results indicated that BAC could significantly improve depression-like behaviors caused by CUMS; however, there was no significant difference between the effects of BPT-SD and BAC.

3.12 Limitations of the study

Preparation of BPT-SD is often difficult because of the non-uniform mixing with the plasticizer TPGS, which is usually waxy and semi-solid at room temperature attributable to its low melting point. The process can be performed on ice with a mortar and pestle to ensure even mixing. For evaluating pharmacodynamics, the behavioral gap between BAC and its solid dispersion is not very evident. This needs to be further investigated to elucidate depression-related indicators in the brain (such as the amount of dopamine and serotonin) by experiments such as western blotting. Further, this can help to explore the differences of the effects of BAC and BPT-SD on the expression of related proteins in the brain.

4. Conclusions

In our study, PVP VA64 was selected as the carrier, and TPGS was used as a plasticizer to prepare BPT-SD, which can improve the dissolution rate of BAC, thereby increasing its oral bioavailability. The HME process is a new, environmentally friendly, and efficient preparation method, that can render BAC highly dispersed in the carrier and maintain good physical stability. This study can improve the dissolution of BAC, inhibit the P-glycoprotein efflux of BAC, and provide a reference for TPGS as a plasticizer and efflux inhibitor to prepare solid dispersions by HME.

Author Statement

Meng Tong: Writing - Original Draft; Writing - Review & Editing; Investigation

Xiaoyan Wu: Writing - Review & Editing; Formal analysis

Shuya Zhang: Validation; Software; Methodology

Di Hua: Data Curation; Writing - Original Draft; Resources

Shukun Li: Validation; Formal analysis; Investigation

Xiangyu Yu: Investigation; Formal analysis;

Jing Wang: Conceptualization; Funding acquisition; Writing - Review & Editing

Zhenhai Zhang: Conceptualization; Funding acquisition; Writing - Review & Editing

Declaration of competing interests

The authors report no conflicts of interest in this work.

Acknowledgments

Funding: This work was supported by the National Natural Science Foundation of China [grant number 81803756]; the Six Talent Peak Projects in Jiangsu Province [grant number SWYY-010-2019]; Construction Projects of Nursing Preponderant Discipline at Nanjing University of Chinese Medicine [grant number 2019YSHL123]; Independent Research Project of Jiangsu Academy of Traditional Chinese Medicine [grant number BM2018024-2019006]; and Jiangsu Medical Innovation Team [grant number CXTDB2017003].

References

Adler, C., Schnenberger, M., Teleki, A.Kuentz, M. 2016. Molecularly designed lipid microdomains for solid dispersions using a polymer/inorganic carrier matrix produced by hot-melt extrusion. Int J Pharm, 499(1-2), 90-100. https://doi.org/10.1016/j.ijpharm.2015.12.057

Beig, A., Fine-Shamir, N., Porat, D., Lindley, D., Dahan, A., 2017. Concomitant solubility-permeability increase: Vitamin E TPGS vs. amorphous solid dispersion as oral delivery systems for etoposide. Eur J Pharm Biopharm. 121, 97. https://doi.org/10.1016/j.ejpb.2017.09.012

Cai, L., Qin, X., Xu, Z., Song, Y.Chen, J. 2019. Comparison of Cytotoxicity Evaluation of Anticancer Drugs between Real-Time Cell Analysis and CCK-8 Method. ACS Omega, 4(7), 12036-12042. https://doi.org/10.1021/acsomega.9b01142

Collnot, E. M., Baldes, C., Schaefer, U. F., Edgar, K. J., Wempe, M. F.Lehr, C. M. 2010. Vitamin E TPGS P-glycoprotein inhibition mechanism: influence on conformational flexibility, intracellular ATP levels, and role of time and site of access. Molecular Pharmaceutics, 7(3), 642-651. https://doi.org/advices10.1021/mp900191s

Collnot, E. M., Baldes, C., Wempe, M. F., Kappl, R., Hüttermann, J., Hyatt, J. A., Edgar, K. J., Schaefer, U. F.Lehr, C. M. 2007. Mechanism of inhibition of P-glycoprotein mediated efflux by vitamin E TPGS: influence on ATPase activity and membrane fluidity. Molecular Pharmaceutics, 4(3), 465. https://doi.org/advices10.1021/mp060121r

Childs, S. L., Kandi, P.Lingireddy, S. R. 2013. Formulation of a Danazol Cocrystal with Controlled Supersaturation Plays an Essential Role in Improving

Bioavailability. Mol Pharm, 10(8), 3112-3127. https://doi.org/10.1021/mp400176y

Fule, R., Paithankar, V.Amin, P. 2016. Hot melt extrusion based solid solution approach: Exploring polymer comparison, physicochemical characterization and in-vivo evaluation. %J International Journal of Pharmaceutics, 280-294. https://doi.org/10.1016/j.ijpharm.2015.12.062.

Fan, W., Zhang, X., Zhu, W.Di, L. 2020. The Preparation of Curcumin Sustained-Release Solid Dispersion by Hot-Melt Extrusion—II.Optimization of Preparation Process and Evaluation In Vitro and In Vivo. J Pharm Sci, 109(3). https://doi.org/10.1016/j.xphs.2019.11.020

He, X., Pei, L., Tong, H. H. Y.Zheng, Y. 2011. Comparison of Spray Freeze Drying and the Solvent Evaporation Method for Preparing Solid Dispersions of Baicalein with Pluronic F68 to Improve Dissolution and Oral Bioavailability Aaps Pharmscitech, 12(1). https://doi.org/advices10.1208/s12249-010-9560-3.

Huang, D., Xie, Z., Rao, Q., Liamas, E., Pan, P., Guan, S., Zhang, Z. J., Lu, M.Li, Q. 2019. Hot melt extrusion of heat-sensitive and high melting point drug: Inhibit the recrystallization of the prepared amorphous drug during extrusion to improve the bioavailability. Int J Pharm, 565, 316-324. https://doi.org/ 10.1016/j.ijpharm.2019.04.064

Huang, R., Han, J., Wang, R., Zhao, X., Qiao, H., Chen, L., Li, W., Di, L., Zhang, W.Li, J. 2019. Surfactant-free solid dispersion of BCS class IV drug in an amorphous chitosan oligosaccharide matrix for concomitant dissolution in vitro - permeability increase. Eur J Pharm Sci, 130:147-155. https://doi.org/ 10.1016/j.ejps.2019.01.031

Huang, Y., Zhang, B., Gao, Y., Zhang, J.Shi, L. 2014. Baicalein–Nicotinamide Cocrystal with Enhanced Solubility, Dissolution, and Oral Bioavailability. J Pharm Sci, 103(8), 2330-2337. https://doi.org/ 10.1002/jps.24048

Ke, W. T., Lin, S. Y., Ho, H. O.Sheu, M. T. 2005. Physical characterizations of microemulsion systems using tocopheryl polyethylene glycol 1000 succinate (TPGS) as a surfactant for the oral delivery of protein drugs. J Control Release, 102(2), 489-507. https://doi.org/ 10.1016/j.jconrel.2004.10.030.

Kim, J. S., Kim, M. S., Park, H. J., Jin, S. J., Lee, S.Hwang, S. J. 2008. Physicochemical properties and oral bioavailability of amorphous atorvastatin hemi-calcium using spray-drying and SAS process. International journal of pharmaceutics, 359(1-2), 211-219. https://doi.org/10.1016/j.ijpharm.2008.04.006.

Kotani, A., Kojima, S., Hakamata, H.Kusu, F. 2006. HPLC with electrochemical detection to examine the pharmacokinetics of baicalin and baicalein in rat plasma after oral administration of a Kampo medicine. Anal Biochem, 350(1), 99-104. https://doi.org/ 10.1016/j.ab.2005.11.007.

Lai, M. Y., Hsiu, S. L., Tsai, S. Y., Hou, Y. C.Chao, P. 2010. Comparison of metabolic pharmacokinetics of baicalin and baicalein in rats. J Pharm Pharmacol, 55(2), 205-209. https://doi.org/ 10.1211/002235702522.

Li, M., Meng, Y., Chu, B., Shen, Y.Xie, Z. 2020. Orexin-A aggravates cytotoxicity

and mitochondrial impairment in SH-SY5Y cells transfected with APPswe via p38 MAPK pathway. Ann Transl Med, 8(1), 5-5. https://doi.org/ 10.21037/atm.2019.11.68.

Li, Y., Lv, O., Fenggang, Qingsong, Z., Zhichao, L.Wu. 2015. Linalool Inhibits LPS-Induced Inflammation in BV2 Microglia Cells by Activating Nrf2. Neurochem Res, 40(7):1520-5. https://doi.org/ 10.1007/s11064-015-1629-7.

Liu, J., Qiu, L., Gao, J.Yi, J. 2006. Preparation, characterization and in vivo evaluation of formulation of baicalein with hydroxypropyl-β-cyclodextrin. International journal of pharmaceutics, 312(1-2), 137-143. https://doi.org/advices 10.1016/j.ijpharm.2006.01.011

Liu, X.Liu, C. 2017. Baicalin ameliorates chronic unpredictable mild stress-induced depressive behavior: Involving the inhibition of NLRP3 inflammasome activation in rat prefrontal cortex. Int Immunopharmacol, 48:30-34. https://doi.org/ 10.1016/j.intimp.2017.04.019.

Nepal, P. R., Han, H.-K.Choi, H.-K. 2010. Enhancement of solubility and dissolution of Coenzyme Q10 using solid dispersion formulation. Int J Pharm, 383(1-2):147-53. https://doi.org/ 10.1016/j.ijpharm.2009.09.031.

Pan, Y., Hong, Y., Zhang, Q. Y.Kong, L. D. 2013. Impaired hypothalamic insulin signaling in CUMS rats: restored by icariin and fluoxetine through inhibiting CRF system. Psychoneuroendocrinology, 38(1), 122-134. https://doi.org/10.1016/j.psyneuen.2012.05.007.

Repka, M. A.,McGinity, J. W. 2000. Influence of Vitamin E TPGS on the properties of hydrophilic films produced by hot-melt extrusion. Int J Pharm, 202(1-2):63-70. https://doi.org/ 10.1016/s0378-5173(00)00418-x.

Shen, X., Zhao, C., Lu, J.Guo, M. 2018. Physicochemical properties of whey protein-stabilized astaxanthin nanodispersion and its transport via Caco-2 monolayer. J Agric Food Chem, 66(6):1472-1478. https://doi.org/ 10.1021/acs.jafc.7b05284.

Slütter, B., Plapied, L., Fievez, V., Sande, M. A., Rieux, A. D., Schneider, Y. J., Riet, E. V., Jiskoot, W.Préat, V. 2009. Mechanistic study of the adjuvant effect of biodegradable nanoparticles in mucosal vaccination. J Control Release, 138(2), 113-121. https://doi.org/ 10.1016/j.jconrel.2009.05.011.

Qian, M., Tang, S., Wu, C., Wang, Y., He, T., Chen, T.Xiao, X. 2015. Synergy between baicalein and penicillins against penicillinase-producing Staphylococcus aureus. Int J Med Microbiol, 305(6), 501-504. https://doi.org/ 10.1016/j.ijmm.2015.05.001.

Wu, C., Xin, P., Liu, X., Lin, L., Pang, H., Li, Y., Guo, Z.Ming, L. 2014. Application of Hot Melt Extrusion for Poorly Water-Soluble Drugs: Limitations, Advances and Future Prospects. Curr Pharm Des, 20(3), -. https://doi.org/advices10.2174/13816128113199990402

Wang, R., Han, J., Jiang, A., Huang, R., Fu, T., Wang, L., Zheng, Q., Li, W.Li, J. 2019. Involvement of metabolism-permeability in enhancing the oral bioavailability of curcumin in excipient-free solid dispersions co-formed with piperine %J International Journal of Pharmaceutics. 561.

https://doi.org/advices10.1016/j.ijpharm.2019.02.02

Wang, W., Cui, C., Li, M., Zhang, Z.Lv, H. 2017. Study of a novel disintegrable oleanolic acid-polyvinylpolypyrrolidone solid dispersion. Drug Dev Ind Pharm, 43(7), 1178-1185. https://doi.org/ 10.1080/03639045.2017.1301950.

Wen, L., Jiaxin, P., Ying, Z., Xutong, M., Bing, Z., Shuya, W., Dongli, Q., Nan, L., Pan, G.Zhidong, L. 2018. A strategy to improve the oral availability of baicalein: The baicalein-theophylline cocrystal. Fitoterapia, 129, 85-93. https://doi.org/ 10.1016/j.fitote.2018.06.018.

Willner, P., Towell, A., Sampson, D., Sophokleous, S.Muscat, R. 1987. Reduction of sucrose preference by chronic unpredictable mild stress, and its restoration by a tricyclic antidepressant. Psychopharmacology, 93(3), 358-364. https://doi.org/ 10.1007/bf00187257.

Xiaoyan, W., Weihong, G., Tengfei, S., Weijun, W., Jian, H., Li, C., Jing, W.Zhenhai, Z. 2017. Enhancing the oral bioavailability of biochanin A by encapsulation in mixed micelles containing Pluronic F127 and Plasdone S630. Int J Nanomedicine, 12, 1475-1483. https://doi.org/ 10.2147/IJN.S125041.

Yu, X., Liu, Y., Wang, Y., Mao, X., Zhang, Y.Xia, J. 2018. Baicalein induces cervical cancer apoptosis through the NF-κB signaling pathway. Mol Med Rep, 17(4):5088-5094. https://doi.org/ 10.3892/mmr.2018.8493.

Zandi, K., Teoh, B.-T., Sam, S.-S., Wong, P.-F.Rais, M. 2012. Novel antiviral activity of baicalein against dengue virus. BMC Complement Altern Med, 12:214. https://doi.org/ 10.1186/1472-6882-12-214.

Zhang, C. Y., Zeng, M. J., Zhou, L. P., Li, Y. Q., Zhao, F., Shang, Z. Y., Deng, X. Y., Ma, Z. Q., Fu, Q., Ma, S. P.Qu, R. 2018. Baicalin exerts neuroprotective effects via inhibiting activation of GSK3β/NF-κB/NLRP3 signal pathway in a rat model of depression. Int Immunopharmacology, 64, 175-182. https://doi.org/ 10.1016/j.intimp.2018.09.001.

Zhang, R., Guo, L., Ji, Z., Li, X., Zhang, C., Ma, Z., Fu, Q., Qu, R.Ma, S. 2018. Radix Scutellariae Attenuates CUMS-Induced Depressive-Like Behavior by Promoting Neurogenesis via cAMP/PKA Pathway. Neurochem Res, 43(11), 2111-2120. https://doi.org/ 10.1007/s11064-018-2635-3.

Zhang, X., Yang, Y., Du, L., Zhang, W.Du, G. 2017. Baicalein exerts anti-neuroinflammatory effects to protect against rotenone-induced brain injury in rats. Int Immunopharmacology, 50:38-47. https://doi.org/ 10.1016/j.intimp.2017.06.007.

Zhang, Y., Luo, R., Chen, Y., Ke, X., Hu, D.Han, M. 2014. Application of carrier and plasticizer to improve the dissolution and bioavailability of poorly water-soluble baicalein by hot melt extrusion. AAPS PharmSciTech, 15(3), 560-568. https://doi.org/ 10.1208/s12249-013-0071-x.

Zhang, Z., Chen, Y., Deng, J., Jia, X., Zhou, J.Lv, H. 2014. Solid dispersion of berberine-phospholipid complex/TPGS 1000/SiO_2: preparation, characterization and in vivo studies. Int J Pharm, 465(1-2), 306-316. https://doi.org/ 10.1016/j.ijpharm.2014.01.023.

Graphical abstract